

Testing of Already Existing and Developing New Compaction Equations during Cold Die Compaction of Iron-1.05% Graphite Powder Blends

Miss Hemlata Nayak¹, C. M. Agrawal², Appu Kuttan³, K. S. Pandey⁴

¹Ph.D. Research Scholar, Department of Mechanical Engineering, MANIT, Bhopal 462051, MP, INDIA

²Former Professor, Department of Mechanical Engineering, MANIT, Bhopal 462051, MP, INDIA.

³Director, Maulana Azad National Institute of Technology, Bhopal 462051, MP, INDIA.

⁴Former Professor, Dept. of MME, National Institute of Technology, Tiruchirappalli 620015, T. N.India.

Abstract: Powder Metallurgy (P/M) processing of materials to produce conventional P/M parts involve the compaction of the pre-determined mass of individual elemental, mixed elemental metal powders or alloy powders and or composite powders into green compacts and sintering them under reducing atmosphere and or under other protective coatings, thus, after sintering producing products after mild machining operations. Therefore, compaction represents one of the most important stages in the production of engineering components using the P/M route. However, the physical properties such as density and the stress distribution in the green compacts are determined not only by the properties of the constituents of the powder or the powder blend, but, also by the pressing modes and schedules. Thus, the present investigation pertains to generate experimental data on the compaction behaviour of Fe-1.05% graphite systems with two different iron particle size ranges and two different powder masses in order to highlight the various aspects of compaction and also testing out the already existing compaction equations and search for the new ones. Powder blends of two different iron powder particle size ranges, namely, -106+53 μ m and -150+106 μ m respectively were blended with the required amount of graphite powder of 3 – 5 μ m sizes for a period of 32 hours. Compaction studies have been carried out for two different amounts of both powder blends. The two amounts taken were 65g and 85g respectively. However, the main attempt was made to record the load and the corresponding heights and the top punch displacements for every two tons (0.02MN) of load which was applied in the steps of 0.02MN. Various equations for compaction were attempted empirically and the already existing ones were also tested. Critical analysis of the experimental data and the calculated parameters have resulted into several compaction equations which were arrived at empirically. The regression coefficient 'R²' in each case where compactions equations were empirically obtained was in very much close proximity to unity. However, it has been also confirmed that the data of the present investigation were well taken up by the earlier compactions equations, thus, validating them comprehensively.

Keywords: Compaction, compacts, constants, empirically, equations, graphite, particle size, powder blends.

I. Introduction

It is universally established that compaction is a process of forming metal, nonmetals (oxides, ceramics, composites etc.) individually or blended in required compositions or alloy powder in to a solid mass (compacts) of desired shape with adequate strength in order to withstand the ejection from the tools and subsequent handling up to the completion of the sintering without breakage or damage. However, compaction of metal or non- metal powders in dies is one among the most versatile methods for shaping metal/alloy/ceramic/composite/blended mixtures powders and the same accounts for the bulk of the commercial production. Further, it is accepted beyond any doubt that deformation is one among the major mechanisms of densification with regards to production of high density parts. Both types of deformations such as elastic and plastic are induced to the compacts. However, most of the elastic deformations are recovered, on the removal of the imposed stress from the compact. But, the recently developed dynamic compaction process which exhibits such characteristic features that differentiates it from the traditional powder metallurgy processes. Apart from these, the dynamic compaction is technically carried out by the passage of an intense shock through the powder mass required to be compacted. This shock wave can be generated by detonation of an explosive that surrounds

the powder mass [1]. The passage of shock wave through the powder particle generates intense plastic deformation which occurs principally at the periphery of the powder particles. The combination of the plastic deformation and the friction among the powder particles can lead to elevated temperatures producing localized melting which promotes the formation of effective joints among the particles. Fig.1 shows the various stages of compaction experienced by the powder particles during compaction operation.

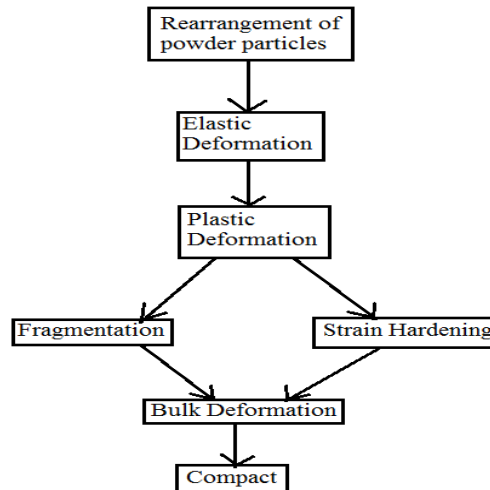


Figure 1 Various Stages Occurring in Powder Compaction

1.1 Compaction Equations

Investigators over the past eighty years have devoted considerable efforts to the development of empirical and theoretical compaction equations to describe the density pressure relationships for the compaction of powders. Even though more than twenty different compaction equations have been proposed of which the most widely used equations are attributed to Balshin[2], Heckel[3] and Kawakita[4] respectively. Some experimental results of investigators have shown that Balshin equation is relatively, too, insensitive to the variation in pressure values at higher ranges and is also not valid in the compaction of ductile powders. However, Heckel and Kawakita equations have shown their applicability to the compaction of both metallic and non-metallic powders [5], but, it has been reported that the Heckel equation is quantitatively invalid at low pressures. These equations are listed beneath:

Balshin Equation: $\ln [p] = -C_1/D + C_2$ ----- (1)

Heckel Equation: $\ln \{1/ (1-D)\} = C_3 + C_4$ ----- (2)

Kawakita Equation: $\{D/ (D-D_0)\} = C_5/P + C_6$ ----- (3)

Where ‘C₁’, ‘C₂’, ‘C₃’, ‘C₄’, ‘C₅’, ‘C₆’ are constants. However, Ge Rongde [6] has developed a new compaction equation not only with excellent accuracy and precision, but, also with the wide applicability. This equation is of the form given below:

Log {ln [(1-D₀)/ (1-D)]} = A log P + B ----- (4)

Where, A and B are empirically determined constants, D₀ is the relative density of the loose powder and ‘D’ is the relative density of the compact. Conventional powder metallurgy processing of materials involve the compaction of metal or alloy powder or composite blended powders or mixed elemental powders of pre-determined mass into green preforms and sintering them under reducing atmosphere or neutral atmosphere as the case may be and, thus, producing the sintered components to required dimensions by mild machining operations. Therefore, the compaction, thus, represents one of the most of important stages in the production of engineering components using the P/M route. However, the physical properties such as density and the stress distribution in the green compacts are determined not only by the pressing schedules and the properties of the constituents of the powders [7]. Thus, the compressibility is one of the most important characteristics of the metal powders since, and it affects the densification processes. Therefore, the compressibility is defined as the ability of the powder to deform under the applied pressure, and, further it is defined as the ratio of the green density of the compact to the apparent density of the given powder mass. However, higher values of compression ratio require greater die depths, but, simultaneously induces several complications due to the

powders introduction of friction between the powder and the die walls and also the internal friction of the powder particles among themselves. Thus, it is reported that the compressibility is dependent on the particle size, shape, porosity and surface properties and their chemical compositions as well [8].

1.2 Some Other Aspects of Compaction

Various other compaction equations relating compaction pressure, green density and green strengths of compacts are discussed in detail elsewhere [9, 10]. However, compaction equations for mono-size spherical powders and their co-ordination number excellently well by J. X. Liu and T. J. Davies [11, 12] in a comprehensive manner. Further a detailed description is available on the relationship between compacting pressures, green densities and the green strengths of compacts used in thermal batteries can be referred elsewhere [13]. Apart from these, the properties of the compacts can be found out in the literature [7, 8, 14] and the mechanical behaviour of powders during compaction and strengths of the compacts can also be referred elsewhere [8, 12, 14-17, 19-21]. Numerical analysis of compaction, simulation and computer modelling of compaction of powders are suitably described in detail elsewhere [13, 18-20]. Some other important aspects of compaction such as die design, enhancement in compressibility of powders and other related phenomenon are also described in the literature [9, 14, 22-25]. Further the role of friction during compaction play a quite significant roles and the same are discussed by other investigators [26, 27]. A new compaction equation for powder materials is proposed by Shujie Li Paul, B. Khosrovabadi and Ben H. Kolster [28]. However, some typical constitutive relationships are, too, found in the literature and the same can be referred elsewhere [29-32]. Viewing all the above complexities, it is, therefore, becomes highly pertinent to investigate the compaction equations, test them and search for the new ones.

II. Experimental Details

2.1 Materials Required and Their Characterization

Materials required to carry out the present investigation successfully were mainly iron powder of two different sizes -106+53 and -150+106, and graphite powder as mixing element and also as lubricant, indigenously designed, manufactured and heat treated die, punch bottom insert and a hollow cylindrical block in order to carry out compaction experiments along with the 1.0MN capacity Universal Testing Machine (UTM). Prior to carrying out the experimental work, the main ingredient iron powder was characterized for chemical purity, apparent density, flow rate and compressibility. The apparent density is defined as the mass per unit volume of loose or unpacked powder. This includes internal pores but excludes external pores. This is basically governed by chemical composition, particle shape, size and size distribution, method of manufacture of metal powder as well as shape and surface conditions [9]. The chemical purity of the iron powder was found to be 99.63% with 0.37% insoluble impurities. Table 1 provides the basic characteristics of iron powder as well as the two powder blends corresponding to Fe-1.05% graphite powders with two different iron powder particle size ranges, namely, -106+53µm and -150+63µm respectively.

Table 1 Basic Characteristics of Iron Powder and Powder Blends

Sl. No.	Systems Investigated	Apparent Density, g/cc	Flow Rate, Sec/100g	Compressibility at a pressure of 420±10 MPa
1	Iron	2.899	55.06	6.589
2	Fe -1.05% graphite; -106+53µm	2.685	47.86	6.367
3	Fe-1.05% graphite; -150+63µm	2.821	45.39	6.554

2.2 Compressibility Data

Compressibility is the measure of the powder ability to deform under applied pressure and is represented by the pressure density or pressure porosity relationship. In order to obtain compressibility data 65 g and 85 g iron powders with 1.05% graphite each appropriately, but, homogeneously blended were separately taken into the die cavity with bottom insert placed were slowly pressed through the punch on 1.0 MN capacity UTM. Loads were applied in the steps of 0.02 MN and the reading such as punch displacement and the actual compact height within the die were calculated so as to calculate the instantaneous density of the compact load. The load was up to 0.28 MN. Prior to compaction studies, the powder blend of iron with a particle size of -150+106µm with 1.05% graphite and also iron particle size of -106+53µm with graphite powder of 3-5µm were blended on a pot mill for a period of 30 hours in order to obtain homogenous blend. From each of the blends 65 g and 85 g were taken for compaction studies. The internal diameter of the mother die was 25+0.01 mm and punch and bottom insert diameters were as 25-0.01 mm. However, during compaction studies, graphite powder paste in acetone was used as a lubricant. The raw data such as the top punch displacement, powder height at

various loads, fractional theoretical density, the applied stress for each height reductions and fractional displacement height reductions were calculated. Based on these calculated parameters various compressibility plots were drawn including testing of most cited compaction equations of Balshin, Heckel, Kawakita and Ge Rong de by introducing their parameters for plotting the graphs. These are highlighted in the results and discussions. The compaction assembly is shown in fig. 2.

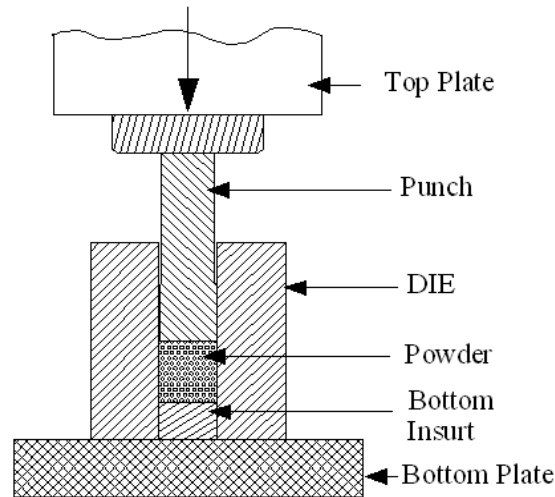


Figure 1 Schematic Diagram of Showing the Complete Powder Compaction Assembly

III. Results and Discussion

Data on compaction of 65 g and 85 g powder blends containing iron 98.95% and 1.05% graphite. Two powder blends were prepared one with iron particle size in the range of -106+53 and another one containing iron particle size in the range of -150+106 μm. Both contained graphite powder particle size in the range of 3-5 μm. Various equations for compaction were empirically arrived at and also already existing compaction equations such as Balshin [(1/D) Vs. (ln P)], Heckel[(1/1-D) Vs. (P)], Kawakita[(D/D-D₀) Vs. (1/P)] and Ge Rong de (Log {ln [(1-D₀)/(1-D)]}) Vs. Log (P) were tested for their validity using the experimental data and calculated parameters.

3.1 Compressibility Plots

Various compressibility plots such as fractional theoretical density vs. load, applied loads and the punch displacements, powder height vs applied loads, applied stress and the fractional displacement height reduction, log (stress) vs. log (h₀/h_c), log (stress) versus log (% fractional theoretical density), [(1/D) Vs (ln P)], [(1/1-D) Vs (P)], [(D/D-D₀) Vs (1/P)] and (Log {ln [(1-D₀)/(1-D)]}) Vs. log P were plotted and curve fitting techniques were attempted and the best fit curves were critically analyzed and are discussed in subsequent sections and sub-sections in detail so as to arrive at the finite outcome.

3.1.1 Fractional Theoretical Density (FTD) vs Load

Figs.3(a) and 3(b) have been drawn between fractional theoretical density and load for 65g and 85g respectively for both the particle sizes, namely, -106+53 μm and -150+106 μm. the characteristic nature of the curves for both powder weights and both iron practice size ranges were found to be similar. Data for both weights have shown that the batch containing larger iron particle size range densified better than the batch containing finer iron powder particle size ranges. The reason which could be associated to the above observation is that the smaller particle size batch densifying poorly which is due to the high surface area effect consuming the sliding friction, rearrangement in the form of particle rotation, translation and simple fall into cavities and also due to the difficulty introduced by virtue of their non-fragmentation during compaction. These plots are found to conform to a third order polynomial equation of the form:

$$\left(\frac{\rho_f}{\rho_{th}}\right) = A_0 + A_1P + A_2P^2 + A_3P^3 \dots \dots \dots (6)$$

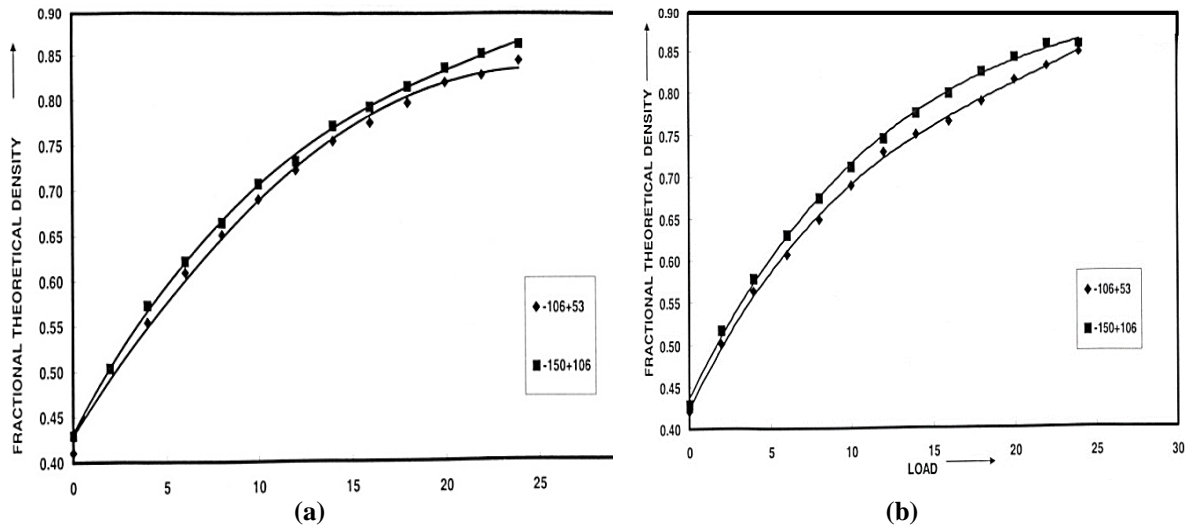


Figure 3 Influence of Iron particle size on the Relationship Between The Fractional Theoretical Density and the Applied Load For Fe-0.65 Graphite During Compaction of (a) 65g Powder Blend (b) 85g Powder Blend

Where, (ρ_f/ρ_{th}) the fractional theoretical density and ‘P’ is the applied load in tons ‘A₀’, ‘A₁’, ‘A₂’, ‘A₃’ are empirically determine constants are found to be dependent upon the powder weights being compacted and also the iron particle size ranges. These constants are listed in the Table 2

Table 2 Coefficients of Third Order Polynomial between Fractional Theoretical Density and Load

Iron powder Particle Size = -106+53µm					
Powder, gm	A ₀	A ₁	A ₂	A ₃	R ²
65	0.4319	0.0386	-0.013	2E-5	0.9993
85	0.4237	0.0393	-0.0015	3E-5	0.9991
Iron powder Particle Size = -150+106µm					
Powder gm	A ₀	A ₁	A ₂	A ₃	R ²
65	0.4291	0.0324	-0.0007	3E-5	0.9961
85	0.4365	0.0393	-0.0013	2E5	0.9971

3.1.2 Relationship between Applied Loads and the Top Punch Displacement

Figs. 4 (a) and 4(b) have been drawn between the load and the top punch displacement showing the influence of the iron particles size ranges for the both 65g and 85g respectively. The characteristics nature of the curves shown in these figs. 4 (a) and 4(b) are found to be similar to each other. These plots further indicate that as the top punch displacement is enhanced, the applied load has also gone up. The largest iron particle size range of powder blend with 1.05% graphite powders during compaction required more loads compared to the smaller iron particle size blend with the same amount of graphite as in the above case during compaction. This is true, for both the powder blend weights 65g and 85g respectively. The curve fitting techniques employed, revealed that all these curves followed an exponential equation of the form:

$$Y = Ae^{bx} \text{----- (7)}$$

Where, ‘Y’ is the applied load and the coefficient ‘A’ and the exponent ‘b’ are empirically determined constants. ‘x’ is the top punch displacement. This equation very well represents all the data points for both the powder blends being compacted with two different powder particles sizes. These constants are tabulated in Table 3.

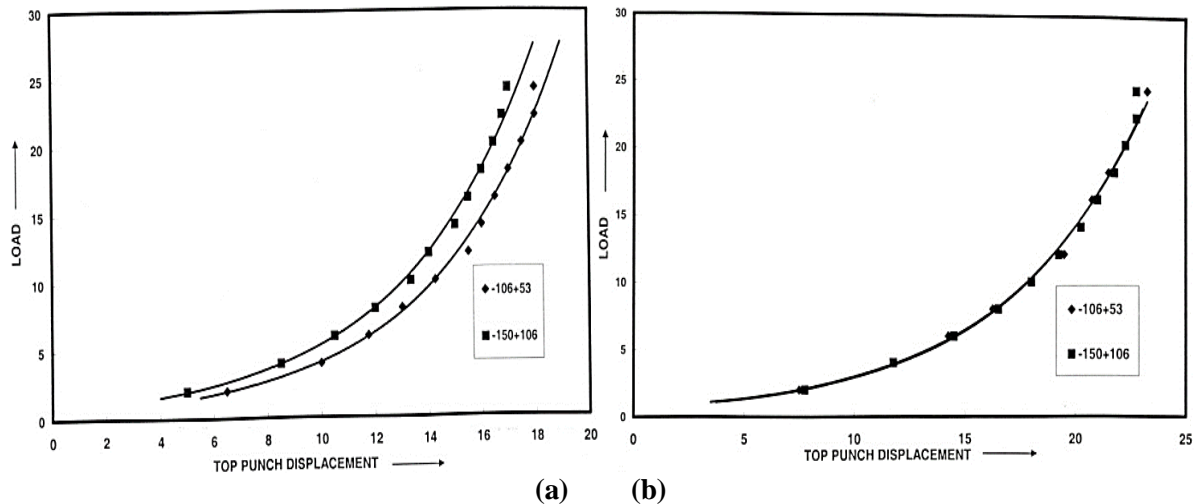


Figure 4 Effect of Iron Particle Size on the Relationship between the Applied Load and the Top Punch Displacement and for Fe-1.05 Graphite Blend during Compaction of (a) 65g (b) 85g

Table 3 Coefficients and Exponents of $Y = A e^{B X}$

Iron Powder Size = -106+53µm			
Powder gm.	A	B	R ²
65	0.4988	0.2129	0.9994
85	0.6403	0.1556	0.9989
Iron Powder Size = -150+106µm			
Powder gm.	A	B	R ²
65	0.6098	0.2043	0.9986
85	0.5987	0.1501	0.9994

3.1.3 Powder Height Vs Applied Loads showing the Influence of Iron Particle Size Ranges

Figs. 5(a) and 5(b) are drawn between powder height and the load applied for both iron particle sizes and also both the powder blends of weights 65g and 85 g respectively. This means 65g and 85 g from first blend with iron particle size of -105+53µm and also 65g and 85 g from the second blend with iron particle size -150+106µm were taken for testing. The characteristic nature of the curve shown in figs. 5(a) and 5(b) are similar in nature irrespective of the iron particle size ranges in each plane. These plots indicate that as the applied load is enhanced, the powder height in each case is decreased. It is also observed that both the particle sizes followed a similar pattern. The empirical relationship that could be established is as under:

$$Y = B_0 + B_1 Z + B_2 Z^2 \text{----- (8)}$$

Where ‘Y’ is the applied load and ‘Z’ is the powder height ‘B₀’, ‘B₁’, and ‘B₂’ are empirically determined constants. The value of ‘B₀’ does not contribute to densification and ‘B₁’ being negative flattens the curve. However positive value of ‘B₂’ contributes to densification. These constants are tabulated in Table 4. Influence of iron particle size ranges have shown virtually no effect on these plots as the curves have virtually merged together.

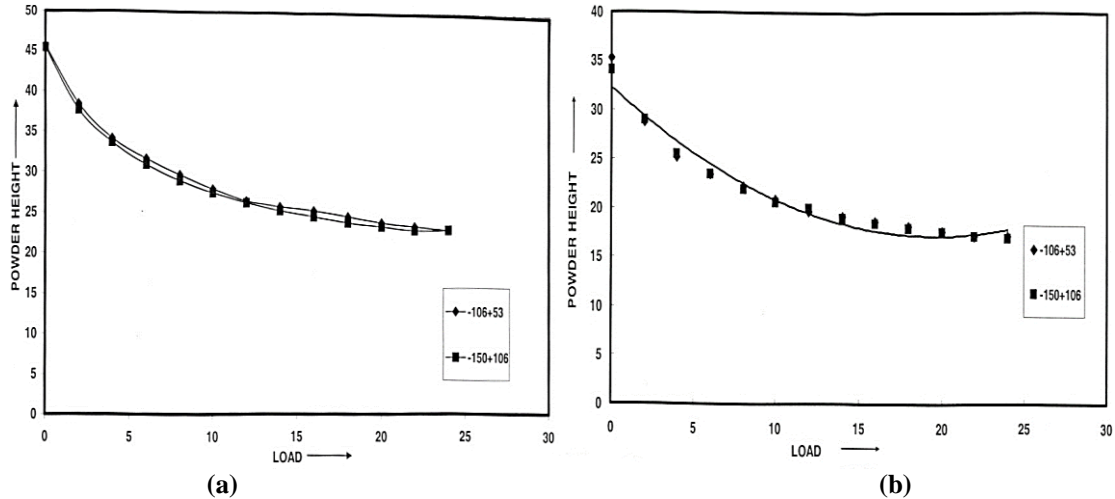


Figure 5 Effect of Iron Particle Size on the Relationship between the Powder Height and the Load for Powder Blend of Fe-1.05% Graphite System (a) 65g and (b) 85g

Table 4 Coefficients of Second Order Polynomial of the Form: $Y=B_0+B_1+B_2X^2$

Powder Particle Size = -106+53μm				
Powder, gm	B ₀	B ₁	B ₂	R ²
65	32.233	-1.532	0.0408	0.9879
85	42.997	-1.998	0.0496	0.9976
Powder Particle Size = -150+106μm				
Powder, gm	B ₀	B ₁	B ₂	R ²
65	32.230	-1.5287	0.0393	0.9994
85	42.599	-2.0499	0.0528	0.9986

3.1.4 Relationship between Applied Stress and the Fractional Displacement Height Reduction

Figs. 6(a) and 6(b) are drawn between the stress and the fractional displacement height reduction. These figures are shown for 65g and 85g of powder blends each with two particle sizes, namely, -106+53μm and -150+106μm respectively. The characteristic nature of the curves indicates that they followed exponential equation. All the data for the plots drawn for different particle size ranges for both powder blends weights, namely, 60g and 80g respectively indicate that for the fixed fractional displacement reduction, the stress required for smaller particle size range, i.e., -106+53μm is higher compared to the stress required for larger particle size, i.e., -150+106μm. This is attributed to the fact that the resistance offered by the smaller particle size range against the applied stress during deformation because of more surface area of the powders of finer size. These plots are found to conform to an exponential equation of the form:

$$\sigma = Ce^{(\frac{Hc}{Ho})q} \text{----- (9)}$$

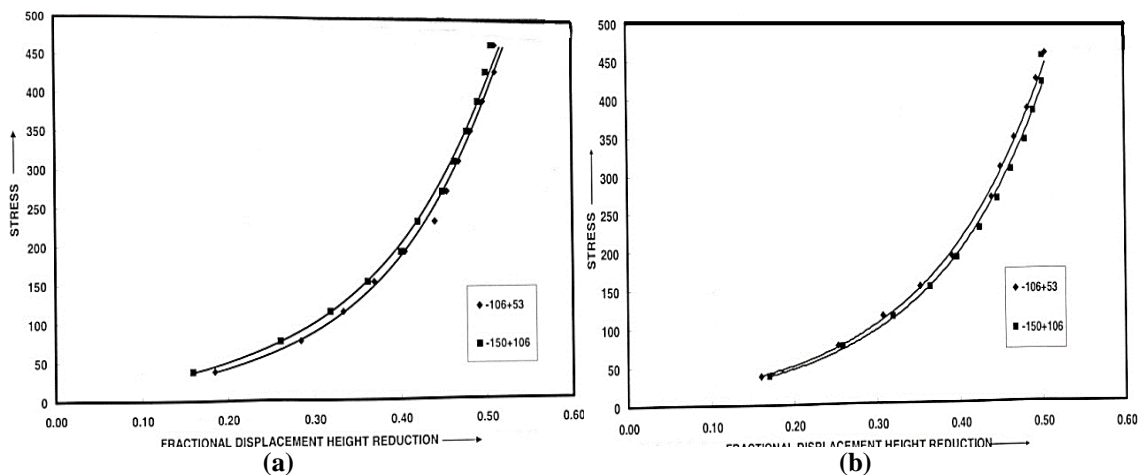


Figure 6 Influence of Iron Particle Size on the Relationship between the Stress and the Fractional Displacement Height Reduction for Fe-1.05% Graphite Blend during Compaction (a) 65g (b) 85g

Where, σ is the applied stress and (H_c/H_0) is the fractional height reduction and ‘C’ and ‘q’ are empirically, determined constants found to be dependent upon the powder weights and the iron particle size ranges used in the present investigation independently into two different sets. Based upon the above observation various logarithmic plots were drawn in the present investigation which are discussed in detail in subsequent sections.

3.2 Logarithmic Plots

Various double logarithmic plots among different parameters were drawn in order to establish possible power law equations among the parameters between whom the double logarithmic plots were drawn. The same are discussed in different sub-headings below:

3.2.1 Log (Stress) Vs. Log (H_0/H_c)

Figs.7(a) and 7(b) have been drawn between $\log(\text{Stress})$ and $\log(H_0/H_c)$ for 65g and 85g powder blend compaction each with two iron particle sizes, i.e., -106+53 μm and 150+106 μm respectively. Fig. 5(a) corresponds to

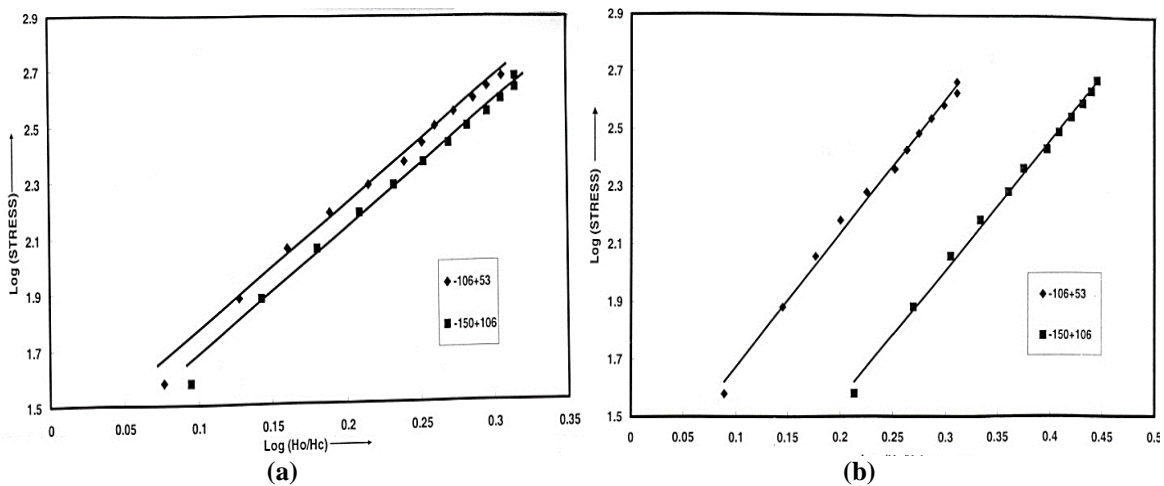


Figure 7 Influence of Iron particle size on the Relationship between the Stress and Height Reduction (H_0/H_c) Ratio for Fe-1.05% Graphite Blend during Compaction of (a) 65g and (b) 85g

65g powder blend compaction, whereas, fig. 5(b) corresponds to 85g powder blend both with two different iron powder particle size ranges in them independently. These plots are found to be perfectly straight lines. This means that they are well represented by a power law equation of the form:

$$(H_0/H_c) = (A) \sigma^m \text{----- (10)}$$

Where, ‘A’ and ‘m’ are empirically determined constants and are found to be dependent upon the iron particle size ranges used in the blend with the graphite powder. These constants ‘A’ and ‘m’ along with the values of the regression coefficients (R^2) are listed in Table 6.

Table 6 Coefficients of the Power Law Equation of the Form: $(H_0/H_c) = A \sigma^m$

Powder weights, g	Iron Powder Particle Size = -106+53 μm		
	A	M	R ²
65	4.6242	1.2116	0.9973
85	4.6019	1.2709	0.9938
Iron Powder Particle Size = -150+106 μm			
65	4.4539	0.6700	0.9993
85	4.3218	0.8024	0.9981

3.2.2 Log (stress) versus Log (% Fractional Theoretical Density)

Figs.8 (a) and 8 (b) have been drawn between $\log(\text{stress})$ and $\log(\% \text{ fractional theoretical density})$. Each of these figs.8 (a) and 8 (b) demonstrate the influence of iron particle size for the given weights, i.e., 65g and 85g respectively. While examining these figs. 8 (a) and 8 (b) respectively, it is observed that the influence

of iron particle size is more pronounced in the case of fig. 8 (b) with 85g of powder blend compaction. These straight lines clearly demonstrate

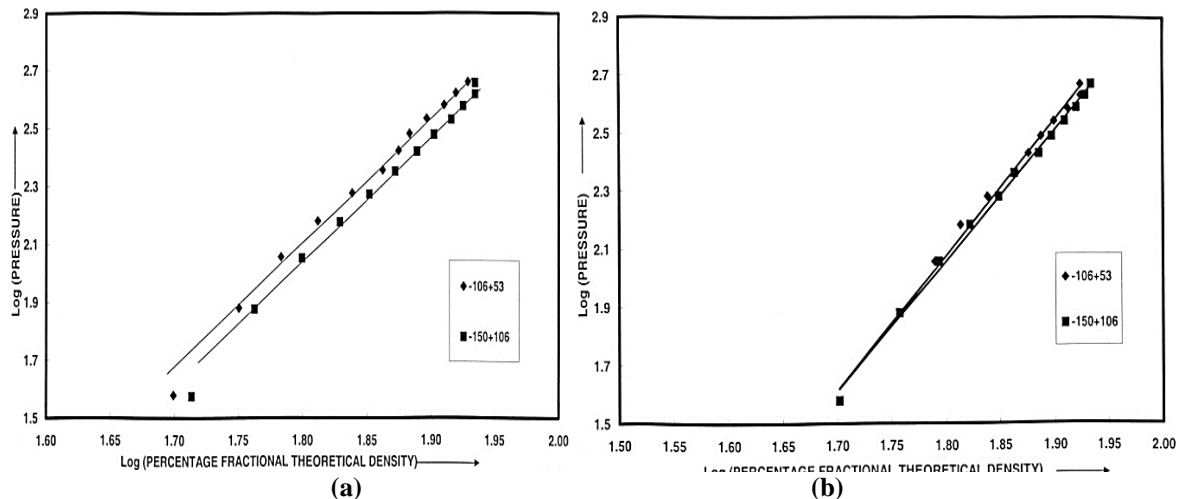


Figure 8 Influence of Iron particle size on the Relationship between Pressure and Fractional Theoretical Density through Log-Log Plots for Applied Load of Powder Blend of Fe-0.65 Graphite during Cold Compaction (a) of 65g (b) of 85g

The influence of iron particle size on the compaction behaviour of Fe-1.05% graphite blends as shown for the given weights, i.e., 65g and 85g respectively. These straight lines clearly indicate that the variables pressure (stress) is linked with the power law relationship with the percent fractional theoretical density. The relationship that empirically exists between the above parameters can be expressed as given underneath:

$$\% (\rho_f/\rho_{th}) = W (\sigma)^p \text{----- (11)}$$

Where, (ρ_f/ρ_{th}) is the fractional theoretical density, 'σ' is the applied stress, 'W' and 'p' are empirically determined constants. These constants are given in Table 7.

Table 7 Coefficients and Exponents of Power Law Equation of the Form: $\% (\rho_f/\rho_{th}) = W \sigma^p$

Powder Weights in g.	Iron Powder Particle Size = -106+53μm		
	W	P	R ²
65	4.6238	-6.2478	0.9944
85	4.4031	-6.1247	0.9981
Powder Weights in g.	Iron Powder Particle Size = -150+106μm		
	W	P	R ²
65	4.4543	-5.9614	0.9964
85	4.3217	-6.1685	0.9961

3.3 Testing of the Existing Compaction Equations

This section deals with the testing of already existing, but, major compaction equations such as Balshin [2], Heckel [3], Kawakita [4] and Ge Rong de [5] in a systematic manner using the experimental and calculated parameters of the present investigation. These are exclusively discussed in the following sub-sections:

3.3.1 Testing of Balshin Equation

Plots were drawn between the inverse of the relative density and ln (pressure) for 65g and 85g powder blends respectively during compaction. Two powder blends of 65g each independently having iron particle size ranges of -106+53μm and another are with -150+106μm. Similar was the case for 85g powder blend. These plots are shown in figs. 9(a) and 9(b) respectively. Influence of iron particle size is distinct in case of 85g powder blend being compacted.

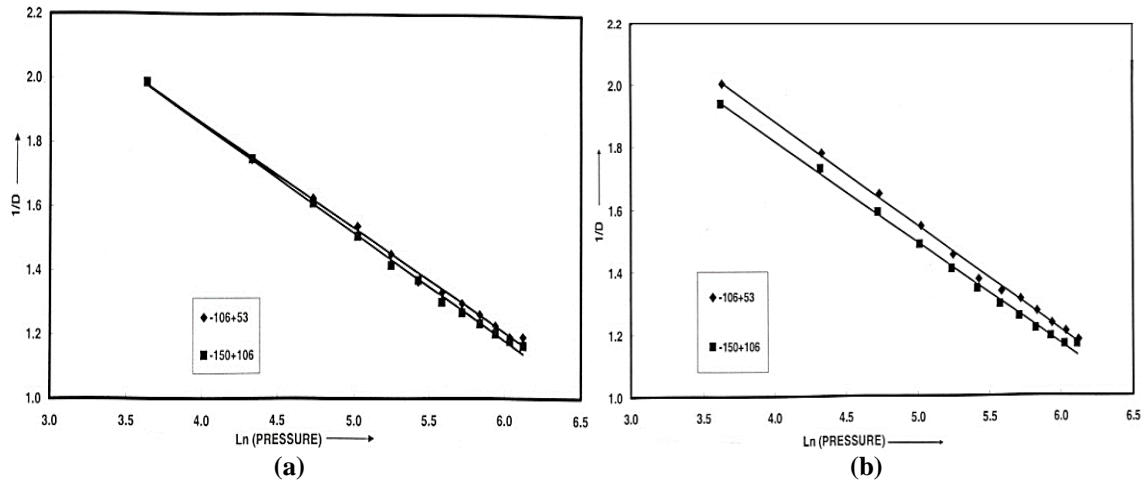


Figure 9 Influence of Iron particle size on the Relationship Between (1/D) and ln (Pressure) for the Applied Load to Powder Blend of Fe-1.05% Graphite during Cold Compaction (a) of 65g (b) 85g

Since the plots shown in these figs. 9(a) and 9(b) respectively are straight lines indicating an absolute adherence to the equation of the form:

$$\ln(P) = C_1/D + C_2 \text{----- (12)}$$

This is the Balshin equation which is validated in totality. The constants ‘C₁’ and ‘C₂’ along with the regression coefficients R² are tabulated in Table 8.

Table 8 Coefficients of Compaction Equation $\ln(p) = C_1/D + C_2$ (Balshin Equation).

Powder weights, g	Iron Powder Particle Size = -106+53µm		
	C ₁	C ₂	R ²
65	-0.3276	3.1701	0.9972
85	-0.3358	3.2228	0.9978
	Iron Powder Particle Size = -150+106µm		
65	-0.3376	3.2045	0.9977
85	-0.3244	3.1125	0.9973

3.3.2 Testing of Heckel Equation

Figs. 10 (a) and 10 (b) are drawn between ln (1/(1-D)) and the pressure for 65g and 85g of powder blend compaction. Both these plots indicate the influence of iron particle size. Since both plots indicate straight lines and quite explicit while showing the influence of iron particle size ranges. All data points for each of the powder blend masses with independent iron particle size ranges corresponded to separate straight lines in conformity with the Heckel Equation. Hence, it was concluded that the data points obtained in the present investigation well conformed to the

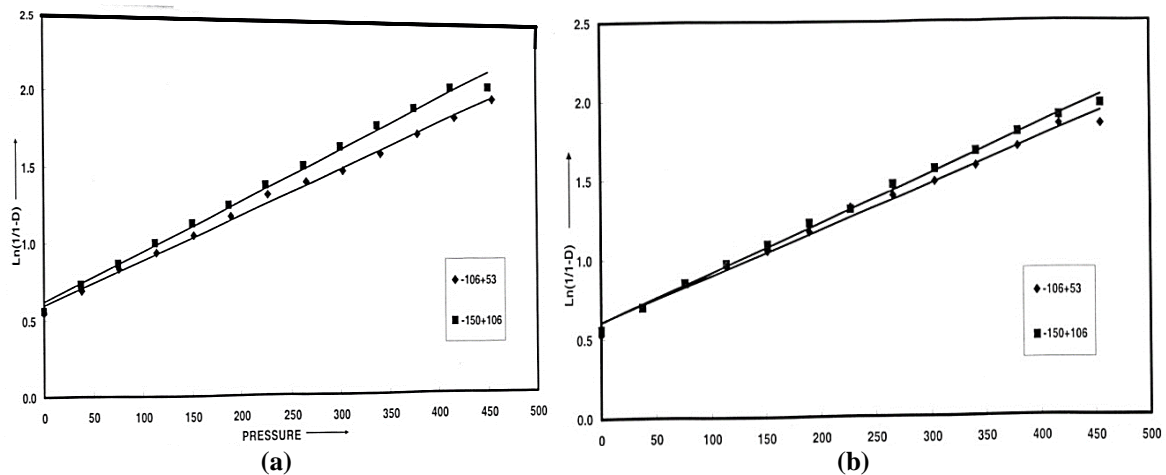


Figure 10 Influence of Iron particle size on the Relationship between Ln (1/(1-D)) and Pressure (P) for Fe-1.05% Graphite Powder Blend during Cold Compaction of Two Different Weights (a) 65g (b) 85

Table 9 Coefficients of the Linear Equation of the form $\ln \{1/ (1-D)\} = C_3 P + C_4$

Powder weights, g	Iron Powder Particle Size = -106+53 μ m		
	C ₅	C ₆	R ²
65	0.0290	0.6083	0.9907
85	0.0290	0.5961	0.9958
Iron Powder Particle Size = -150+106 μ m			
65	0.0031	0.6064	0.9966
85	0.0032	0.6196	0.9934

HeckelEquation of the form is given below:

$$\ln \{1/1-D\} = C_3 P + C_4 \text{ ----- (13)}$$

Where, the constants ‘C₃’ and ‘C₄’ are empirically determined and the same are tabulated in Table 9 along with the values of the regression coefficients, ‘R²’. The values of the regression coefficients ‘R²’ are found to be in extremely close proximity to unity, hence, the curve fittings are almost near to perfection. Therefore, Heckel equation of compaction is very well validated.

3.3.4 Testing of Kawakita Equation

Figs. 11 (a) and 11 (b) are drawn between $\{D/ (D-D_0)\}$ and the inverse of pressure, i.e., $\{1/P\}$ showing the influence of iron particle size in both the case. A distinct effect of iron particle size on the relationship is seen. In both the cases, the convergence is virtually at the same point from where the divergence in 85g powder blend is more predominant. Since these plots are typically straight lines, and, thus, validating the Kawakita equation almost cent per cent.

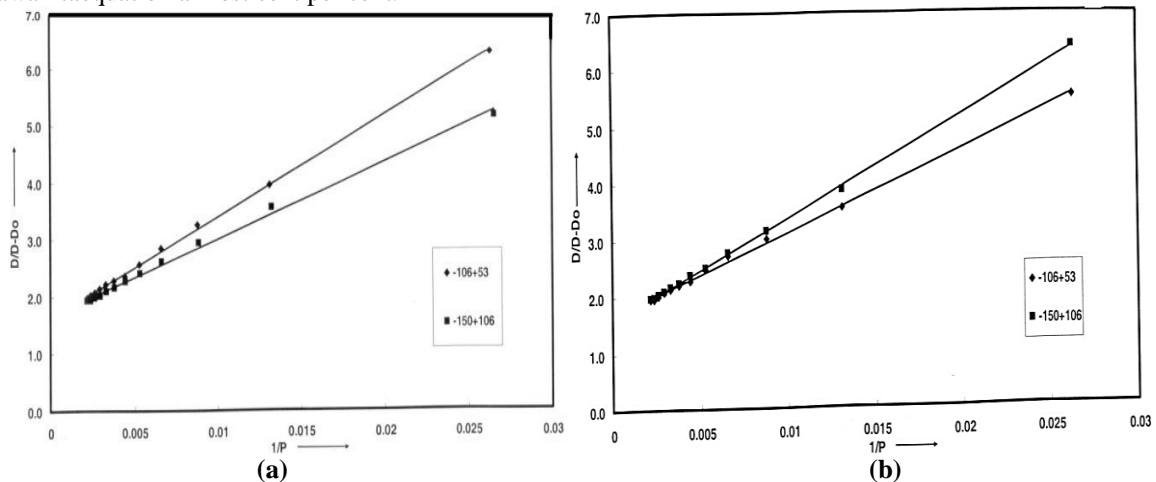


Figure 11 Plots Showing Relationship between $\{D/ (D-D_0)\}$ & $\{1/ \text{Pressure}\}$ Fe-1.05% Graphite with Iron Powder Particle Size of -106+53 μ m, -150+106 μ m. (a) of 65g Weight (b) of 85g Weight $\{D / (D-D_0)\} = C_5 (1/p) + C_6$

Where, ‘C₅’ and ‘C₆’ are empirically determined constants. These constants along with the value of the regression coefficients ‘R²’ are given in Table 10.

Table 10 Coefficients of linear equation of the form: $\{D/ (D-D_0)\} = C_5 (1/P) + C_6$

Powder weights	Iron Powder Particle Size = -106+53 μ m		
	C ₅	C ₆	R ²
65	143.23	1.6664	0.9978
85	176.69	1.6246	0.99972
Iron Powder Particle Size = -150+106 μ m			
65	178.39	1.5614	0.9995
85	132.73	1.6717	0.9953

3.3.5 Testing of Ge Rong de Compaction Equation

Figs.12 (a) and 12 (b) are drawn between $\log \ln \{1-D_0\}/(1-D)\}$ and $\text{Log}(p)$ showing the influence of iron particle size ranges for two powder bend weighs, namely 65g and 85g respectively. Fig.12 (a) shows the intermingling effect of the iron particle sizes whereas fig.12 (b) distinctly shows the effect. The line corresponding to lower iron particle (-100+53 μ m) size range is below the line corresponding to line of higher

particle size of iron powder in the range of (-150+186µm). Since in both figs. 10 (a) and 12 (b), a straight line relationship is shown. Hence, they corresponded to the following straight line equation of the form:

$$\ln \{(1-D) / (D-D_0)\} = A \log (P) + B \text{ ----- (14)}$$

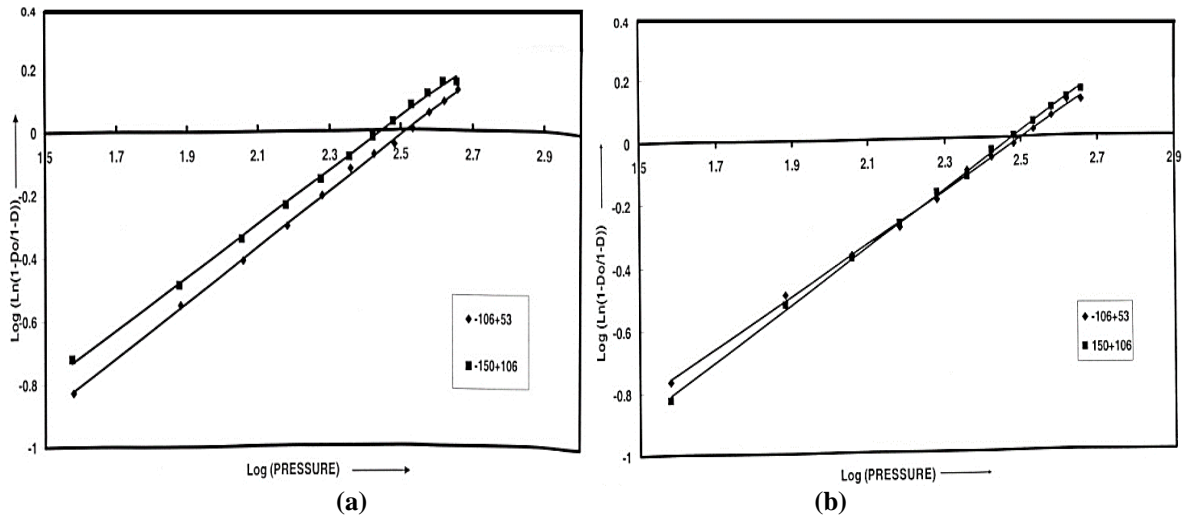


Figure 12 Plots Showing Relationship Between $\log[\ln(1-D_0/1-D)]$ and $\log(\text{Pressure})$ Fe-1.05% C Systems for Iron Powder Particle Size Ranges of -106+53µm, -150+106µm respectively for (a) 65gm (b) 85g.

The values of these constants ‘A’ and ‘B’ along with the values of the regression coefficients ‘R²’, are given in Table 11. Since, the values of the regression coefficient ‘R²’ in each case is in very much close proximity to unity, and, therefore, the curve fitting is excellent and, hence the Ge Rong de equation is fully validated.

Table 11 Coefficients of linear equation of the form $\ln \{(1-D)/(D-D_0)\} = A \log (P) + B$

Powder weights	Iron Powder Particle Size = -106+53µm		
	A	B	R ²
65	0.9004	-2.2321	0.9990
85	0.8776	-2.2089	0.9989
Iron Powder Particle Size = -150+106µm			
65	0.8222	-2.0564	0.9978
85	0.8396	-2.0551	0.9987

3.3.6 Log (Density Difference) V/S. Log (pressure)

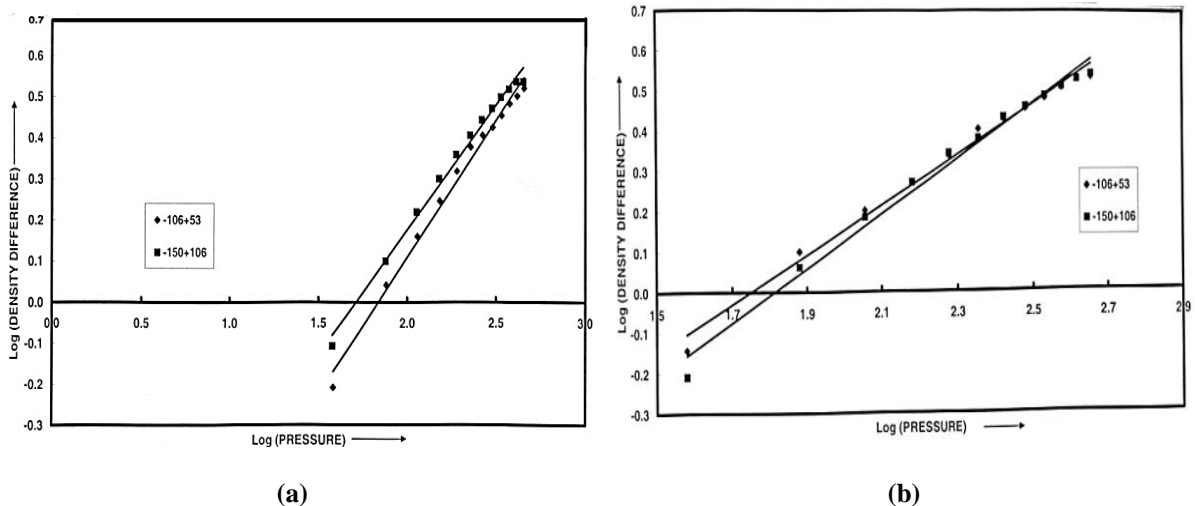


Figure 13 Plots Showing Relationship Between $\log[\ln(\text{Density Difference})]$ and $\log(\text{Pressure})$ Fe-1.05% C System for Powder Particle Size of -106+53µm and -150+106µm. (a) 65gm (b) 85gm

Figs, 13(a) and 13 (b) are drawn between log density difference and log of pressure showing the influence of iron particle size ranges. Fig.13(a) corresponds to 65g powder weight whereas Fig. 13(b) represents the compaction of 85g powder blends respectively. In both these figs. 13(a) and 13(b), the plots represent straight lines for each of the iron particle size ranges, and, hence, the log-log plot showing straight lines amounts to the fact that the density.

Table 12 Coefficients of linear equation of the form $\log(\text{Density Difference}) = S \log(P) + f_0$

Powder weights,g	Iron Powder Particle Size = -106+53µm		
	S	f ₀	R ²
65	0.6093	-10664	0.9995
85	0.6629	-1.2158	0.9904
Iron Powder Particle Size = -150+106µm			
65	0.6689	-1.2132	0.9961
85	0.6041	-10319	0.9925

Difference is proportional to a power of the pressure applied during compaction in such a manner so as to follow the following relationship as given underneath:

$$\text{Density Difference} = f_0 (\text{pressure})^s \text{----- (15)}$$

Where, 'f₀' and 's' are empirically determined constants. The values of these constants along with the values of the regression coefficients are given in Table 12. Thus, $\log(\text{Density Difference}) = S \log(p) + \log(f_0)$. It has been established that all plots made corresponded to a definite equations may it be polynomial or a power law equation. In general the value of the regression coefficient 'R²' has been found very much close to unity in each case, hence, the tested compaction equations were comprehensively validated. Thus, the present investigation provides ample opportunity to researchers for appropriate design of compacts initial density and pressures required during planning to produce P/M components in the sintered conditions or even for structural applications of high densities and high strengths

IV. Conclusions

Based on the critical analysis of the experimental data and the calculated parameters and with the help of series of plots constructed, the main outcomes of the present investigation emerged out are as listed underneath:

1. Fractional theoretical density attained during compaction against the applied loads was established to conform to a third order polynomial of the form: $(\rho_c/\rho_{th}) = A_0 + A_1P + A_2P^2 + A_3P^3$; Where, 'p' is the applied load and 'A₀', 'A₁', 'A₂', and 'A₃' are empirically determined constants found to depend upon the iron particle size ranges and the weights of the powder blends taken for compaction,
2. An exponential relationship of the form: $Y = Ae^{bX}$ has been empirically established between the applied loads and top punch displacements. Where, Y is the applied load, X is the top punch displacement, 'A' and 'b' are empirically determined constants which were found to be dependent upon the iron particle size ranges and the powder blend weights taken for compaction,
3. Empirical relationship between the powder height and the load conformed to a second order polynomial of the form: $Papp = B_0 + B_1Z + B_2Z^2$; Where, 'Papp' is the applied load and Z is the powder height in mm. Further, B₀, B₁, and B₂ are empirically determined constants dependent upon the iron particle size ranges and weights of the powders taken for compaction,
4. Stress (σ) Vs Fractional Displacement, i.e., Fractional Height reduction $\{(H_0 - H_c)/H_0\}$ or $(\Delta H/H_0)$ plots were found to conform to an exponential relationship of the form: $\sigma = C e^{(\Delta H/H_0)^q}$; Where, σ is the applied stress and $(\Delta H/H_0)$ is the fractional height reduction. Whereas, 'C' and 'q' are empirically determined constants. These constants were found to depend upon the powder weights taken for compaction and the iron particle size ranges used in the present investigation,
5. Compact ability (H_c/H_0) was found to be related to the Stress (σ) through a power law equation of the form: $(H_c/H_0) = Q \sigma^m$; Where, 'Q' and 'm' are empirically determined constants and are dependent upon powder blend weights taken for compaction and the iron particle size ranges independently used,
6. Percentage fractional theoretical density (ρ_c/ρ_{th}) is directly proportional to a power of applied Stress (σ) such that: $\%(\rho_c/\rho_{th}) = W \sigma^b$ Where, 'W' and 'b' are empirically determined constants found to depend upon the particle size ranges and weights of the powders taken for compaction, and,

7. Various plots drawn for testing the already existing compaction equations found in the literature which are namely, Balsin, Heckle, Kawakita and Ge Rong De respectively had shown excellent curve fittings. All data points in each case followed a straight line path irrespective of the particle size ranges used and the powder blend weights taken for compaction. The values of the regression coefficient ' R^2 ' in each case was very much in close proximity to unity, and, thus, validating all the compaction equations mentioned above. Further, the values of ' R^2 ' in each case where compaction equations were empirically arrived at were also in very much close vicinity to unity. Hence, the compaction equations proposed in the present investigation are equally valid and simple to use.

REFERENCES

- [1]. R. M. German, "Powder Packing Characteristics" Metal Powder Industries Federation, pp. 222-223.
- [2]. R. Panelli and F. AbbrozioFilho, "Compaction Equations and Its Use to Describe Powder Consolidation Behaviour", Powder Metallurgy, Vol. 41, No.2, pp131-133, 1998.
- [3]. K. J. Kawakita, "Journal of Japan Society", Powder Metallurgy, Vol. 10, pp.236-244, 1963.
- [4]. W.D.Jones, "Fundamental Principles of Powder Metallurgy, 1960, Edward Arnold Ltd. London.
- [5]. Ge Rong de, "A New Powder Compaction Equation", International Journal of Powder Metallurgy, Vol. 27, No. 3, pp.211-214, 1991.
- [6]. K. H. Roll, "Challenges and Opportunities for Powder Metallurgy in Structural Applications", Powder Metallurgy, Vol. No. 25, pp 159-165, 1982.
- [7]. Joshi, J. Wildermuth⁷⁸ and D. F. Stein, "Effect of Impurity Elements on the Properties of Iron P/M Compacts", The International Journal of Powder Metallurgy and Powder Technology, Vol. 11, No. 2, pp, 137-142, 1975.
- [8]. R. M. German, "Strength Dependence on Porosity for P/M Compacts", The International Journal of Powder Metallurgy and Powder Technology, Vol. 13, No. 4, pp, 259-271, 1977.
- [9]. In-Hyung Monn And Kyung-Hyup Kim, "Relationships Between Compacting Pressure, Green Density and Green Strength of Powder Compacts", Powder Metallurgy, Vol. 27, No. 2, pp. 80-84, 1984.
- [10]. M. M. Carroll and K. T. Kim, "Pressure-Density Equations for Porous Metals and Metal Powders", Powder Metallurgy, Vol. 27, No.3, pp. 153-159, 1984. 1987.
- [11]. J. X. Liu and T. J. Davies, "Co-ordination Number-Density Relationship for Random Packing of Spherical Powders", Powder Metallurgy, Vol. 40. No. 1, pp. 48-50, 1997.
- [12]. J. X. Liu and T. J. Davies, "Packaging State and Compaction Equation of Mono-size Spherical Powders", Powder Metallurgy, Vol. 40. No. 1, pp. 51-54, 1997.
- [13]. D. Coube and H. Riedel, "Numerical Simulation of Metal Powder Die Compaction with Special Consideration of Cracking", Powder Metallurgy, Vol. 43. No. 2, pp.123-131, 2000.
- [14]. Kao and M. J. Koczak, "Mixing and Compacting Behaviour of Ferrous Powders", The International Journal of Powder Metallurgy and Powder Technology, Vol. 16, No. 2, pp, 105-121, 1980.
- [15]. M. V. Veidis and K. R. Geiling, "Relationship Between Mechanical Properties and Particle Size of Iron Powder Compacts", The International Journal of Powder Metallurgy and Powder Technology, Vol. 17, No. 2, pp, 135-139, 1981.
- [16]. Y. Morimoto, T. Hayashi and T. Takei, "Mechanical Behaviour of Powders during Compaction In A Mould With Variable Cross-Sections", The International Journal of Powder Metallurgy and Powder Technology, Vol. 18, No. 2, pp, 129-145, 1982.
- [17]. K. T. Kim and J. S. Kim, "Stage I Compaction Behaviour of Tool Steel Powders Under Die Pressing", Powder Metallurgy, Vol. 41. No 3, pp.199-204, 1998.
- [18]. Xue-Kun Sun, Shao-Jie Chen, Jian-Zhong Xu, Li-Dong Zhen and Ki-Tae Kim. "Analysis of Cold Compaction of Metal Powders", Materials Science and Engineering, A267, pp. 43-49, 1999.
- [19]. G. Portal, E. Euvrard, P. Tailhades and A. Rousset, "Relationship Between Compacting Pressure Green Density and Green Strength of Compacts Used in Thermal Batteries", Powder Metallurgy, Vol. 42. No 1, pp.34-40, 1999.
- [20]. P. M. Modnet, "Computer Modelling Group, "Comparison of Computer Models Representing Powder Compaction Process", Powder Metallurgy, Vol. 42. No 4, pp.301-311, 1999.
- [21]. Howard H. Kuhn, "Optimum Die Design for Powder Compaction", The International Journal of Powder Metallurgy and Powder Technology, Vol. 14, No. 4, pp, 259-275, 1978.
- [22]. M. J. Koczak and J. F. McGraw, "A Laboratory Production Compaction of Powder Compacting and Ejection Response", The International Journal of Powder Metallurgy and Powder Technology, Vol. 16, No. 1, pp, 37-54, 1980.
- [23]. R. Angers and A. Couture, "A New Approach to Increasing the Compressibility of Iron Powders", The International Journal of Powder Metallurgy and Powder Technology, Vol. 29. R. Cytermann and R. Geva, "Development of New Model for Compaction of Powders". Powder Metallurgy, Vol. 30, No. 4, pp. 256-260, 1987. 23, No. 2, pp. 83-93, 1987.
- [24]. Rostislav A. Andrievski, "Compaction and Sintering of Ultrafine Powders". The International Journal of Powder Metallurgy, Val, 30, No. 1, pp. 59-66, 1994.
- [25]. David T. Gethin, Viet D. Tran, Roland W. Lewis and Ahmed K. Ariffin, "An Investigation of Powder Compaction Processes", The International Journal of Powder Metallurgy, Val. 30, No. 4, pp. 385-397, 1994.

- [26]. Yukio Sano, Kiyohiro Miyagi and Tatsuzo Hirose, "Influence of Die Wall Friction on the Dynamic Compaction of Metal Powders", *The International Journal of Powder Metallurgy and Powder Technology*, Vol. 14, No. 4, pp, 291-393, 1978.
- [27]. J. Duszezyk and J. Lemanowicz, "Influence of the Rotary Motors of a Die on Friction During Compaction of Iron Powder", *The International Journal of Powder Metallurgy and Powder Technology*, Vol. 16, No. 3, pp, 269-278, 1980.
- [28]. Shujie Li, Paul B. Khosrovabadi and Ben H. Kolster, "A New Compaction Equations for Powder Materials", *The International Journal of Powder Metallurgy and Powder Technology*, Vol. 30, No. 1, pp.47-57, 1987.
- [29]. R. Cytermann and R. Geva, "Development of New Model for Compaction of Powders". *Powder Metallurgy*, Vol. 30, No. 4, pp. 256-260, 1987.
- [30]. Stuart B. Brown and Guillermo G. A. Weber, "A Constitutive Model for the Compaction of Metal Powders", *Modern Developments in Powder Metallurgy*, Vol. 18-21, pp. 465-476, 1988.
- [31]. Kordecki and B. Weglinski, "Theoretical Aspects of Compaction of Di-electromagnetic Powder Metallurgy Materials", *Powder Metallurgy*, Vol. 31, No. 2, pp. 113-116,1988
- [32]. K, Sun and K. T. Kim, "Simulation of Cold Die Compaction Densification Behaviour of Iron and Copper Powders by Cam-Clay Model", *Powder Metallurgy*, Vol. 40. No. 3, pp.193-195, 1997.